Temperature measurements in the air gap of highly insulated wood-frame walls in a Zero Emission Building

Brozovsky, Johannes; Oksavik, Odne; Rüther, Petra

Published in:
NSB 2023 - Book of Technical Papers: 13th Nordic Symposium on Building Physics

DOI (link to publication from Publisher):
10.54337/aau541595903_2

Publication date:
2023

Document Version
Publisher's PDF, also known as Version of record

Temperature measurements in the air gap of highly insulated wood-frame walls in a Zero Emission Building

J Brozovsky, O Oksavik and P Rüther
Architecture, Materials and Structures, SINTEF Community, 7034 Trondheim, Norway

E-mail: johannes.brozovsky@sintef.no

Abstract. Especially for wooden wall constructions, ventilated rain-screen walls have been used for many decades to prohibit moisture-induced damage. The air gap behind the façade cladding provides drainage, enhances ventilation, and thus facilitates drying of wetted façade components. The conditions in the air gap behind different cladding materials, however, are still an object of research. In the presented study, the interim findings after more than two years of ongoing measurements in the air gap behind different cladding materials of a zero-emission office building in the high-latitude city of Trondheim, Norway are presented. The results provide valuable insight into the temperature conditions in the air gap of ventilated claddings in order to determine the in-use conditions of building materials and develop improved testing schemes. The results indicate that the air and surface temperature in the air cavity of the walls is strongly influenced by the solar radiation incidence on the facades. Both the highest and lowest values were observed on the roof with 81 °C and -21.9 °C, respectively, at the back side of the building integrated photovoltaic modules, resulting in a total temperature range of almost 103 °C.

1. Introduction

Especially for wooden wall constructions, ventilated rain-screen walls have been used for many decades to prohibit moisture-induced damage. The air gap behind the façade cladding provides drainage, enhances ventilation, and thus facilitates drying of wetted façade components. However, the conditions in the air gap behind different cladding materials, are still an object of research. For instance, Girma and Tariku [1] investigated the thermal conditions in ventilated air gaps of different depths behind fibre cement cladding in Burnaby, Canada to evaluate their effect on the thermal performance of the wall in summer conditions. Riahinezhad et al. [2] measured the conditions in the ventilated air gap in a test house in Ottawa, Canada, over 6 years. This was done for the surface temperature on both sides of the air gap in a south-facing brick-cladded façade (back of cladding and top of orientated strand board sheathing) and underneath of the roofing underlayment below asphalt shingles in the roof's air gap. They reported the frequency of occurrence by categorizing the hourly-averaged measurements into 5 °C intervals and average monthly temperatures over the measurement period. Geving et al. [3] took detailed measurements of the hygrothermal conditions in ventilated and unventilated air gaps behind wooden cladding in Trondheim, Norway, over the course of 2 years.

These previous works, however, are either only done for short periods of time as in [1], or only for one façade or roof orientation as in [2] and [3]. In this research, the data from the first 2 years of an ongoing measurement campaign in the air gap behind different cladding materials of a zero-emission office building in Trondheim, Norway (63°24′51″ N, 10°24′27″ E) are presented. Preliminary results from the same measurement campaign from November 2019 to February 2020 are shown in an earlier study by Rüther et al. [4] and Brozovsky et al. [5] used the measurements to calibrate a hygrothermal simulation model for future applications. Measurements were taken at in total 21 locations in five different orientations (North, South, East, West, and inclined South-facing roof) of the building envelope with three sensor positions per location: (i) surface of the wind barrier, (ii) middle of the air gap, and (iii) back side of cladding which includes charred wood, building integrated photovoltaics (BIPV), and black aluminium-covered polyethylene (Alu-PE) panels. Thus, in total 63 thermocouples were installed, and the measurements are logged once every 15 minutes starting September 1, 2020.

2. Measurement setup

2.1. ZEB Laboratory

The building that served as a test facility for the experimental data collected in this study is the Zero Emission Building (ZEB) Laboratory (https://zeblab.no). Completed in 2020, the ZEB Laboratory was designed and constructed to provide a research facility allowing for testing new environmentally friendly building components, solutions, strategies, and constructions as well as management processes [6–8]. It is a 4-storey, ca. 2000 m^2 living office laboratory with glued laminated timber columns, cross-laminated timber floors, stiffening internal walls, and insulated wooden framework in the external walls as load-bearing structure. On the façade to the North, charred wood is used as cladding material, BIPV on the roof, and both BIPV and Alu-PE panels on the remaining facades (see figure 1 and figure 2). Unfortunately, no measurements of the optical properties of the cladding materials are available. The determination of which remains subject of further work.

Figure 1. The ZEB Laboratory viewed from the Southeast (a), and Northeast (b). Photos: © Nicola Lolli, 2021.

2.2. Measurements and sensors

There are 21 measurement locations with three sensor positions each, resulting in 63 thermocouples in total. Figure 2 highlights the locations and names of the sensors used in this study, as well as the sensor positions within the air gap. There are in total five sensor locations behind charred wood as façade cladding, 14 behind BIPV, and two behind Alu-PE panels. The wall and roof structures can be seen in figure 3. For this study, measurements starting 01.09.2020 until 31.08.2022 were used. The frequency of logging is 1 every 15 minutes. Thermocouples of type T were used which have a measurement range from -40 to +85 °C and an accuracy of ±0.5 °C, after an initial calibration. Indoor temperature data is not shown in this work. However, most commonly, it was between 20 and 23 °C. Furthermore, because of high insulation thicknesses of the building envelope, it can be reasonably assumed that small changes in indoor air temperature only have a negligible effect on the conditions in the air gap. The roof has a 30° inclination precisely towards South to maximize BIPV production.

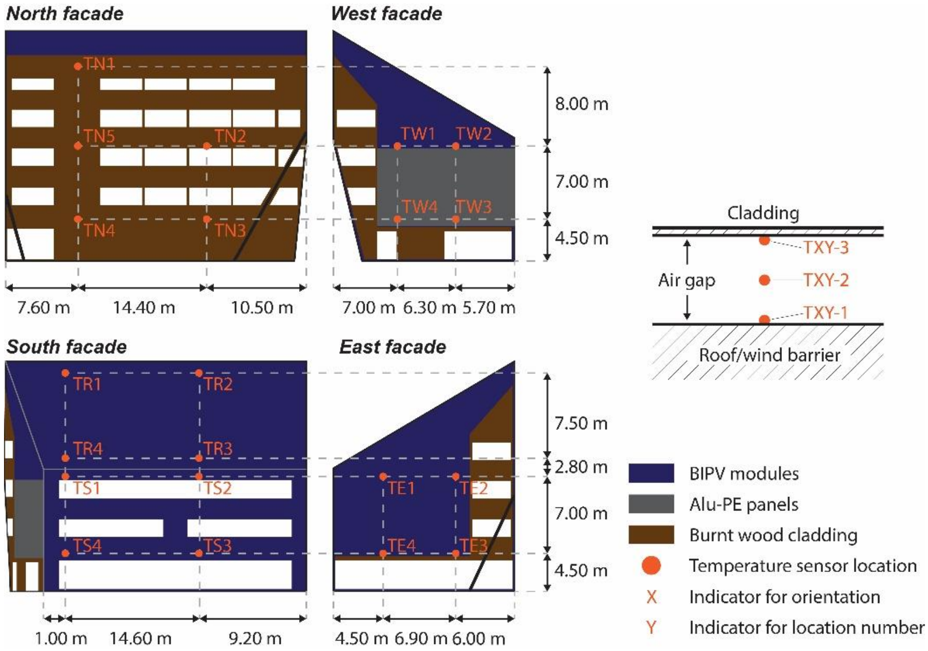

Figure 2. Schematic illustration of the locations of temperature (T) sensors on the five building envelopes north façade (N), east façade (E), south façade (S), west façade (W), and roof (R) and thermocouple positions in the air gap.

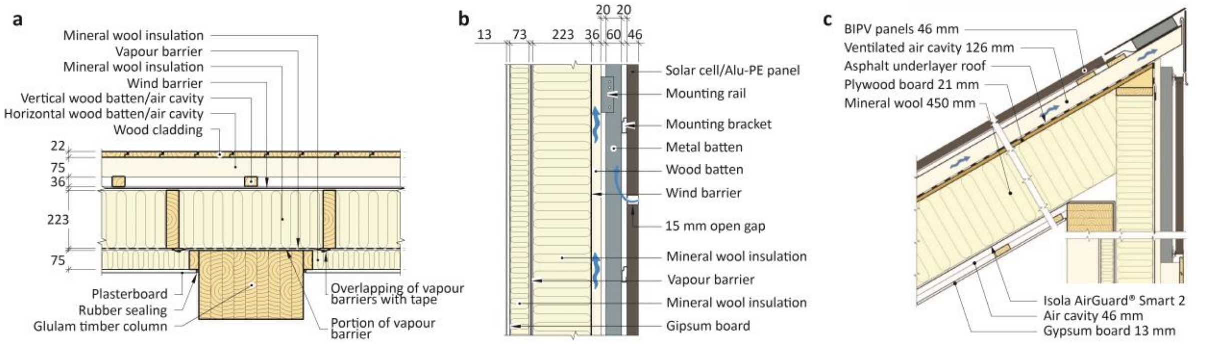

Figure 3. Wall with wood cladding (a), BIPV/Alu-PE panel (b), and BIPV-covered roof (c).

3. Results and discussion

The measured mean hourly temperature in the ventilated air gap ranges from -21.9 °C (*TR2-3* on 11.02.2021 at 07:45 CET) up to 81.0 °C (*TR2-3* on 25.07.2022 at 12:00 CET). Boxplots of the measurements are shown in figure 4. It is noticeable that the *TXY-3* sensors (at the back of the cladding) recorded both the highest and lowest temperatures at the respective locations. This is the case in every location where complete data is available, except for *TR3*. The minimum temperatures at the wind barrier and in the middle of the air gap are almost identical. This is because they are mostly affected by the outdoor air temperature and convection inside the air gap. The recorded temperatures at the back of the cladding, however, are additionally affected by radiative heat losses of the cladding to the surrounding during cold nights. This leads to the cladding material being colder than the ambient air. During times of solar irradiation, the opposite effect can be observed. Then, the cladding material gets heated up by the sun well above ambient air temperature. Due to that, the cladding material emits longwave radiation energy to the wind barrier surface where this radiation is absorbed, and the second highest maximum temperature of a respective location is measured. In the middle of the air gap, the lowest maximum temperature of a respective location is measured, meaning that it is closest to the ambient air temperature. From figure 4, it is also visible that the median of recorded temperatures is highest at the wind barrier and lowest at the back of the cladding of a respective location where complete data is available. However, there are exceptions to that with *TE4*, *TW3* and *TW4*. In *TE4*, the missing data for parts of the measurement period is most likely responsible for this deviation. At the façade to the North, the lowest temperature levels are recorded. At the highest measurement location on this façade (*TN1*), higher temperatures are recorded than at the remaining northern measurement locations due to less shading from surrounding buildings. However, lower heat conductivity of the wood cladding compared to the BIPV and Alu-PE panels might also be a reason for lower temperature levels. At *TR2*, both the absolute maximum and minimum temperatures are recorded, resulting in a total temperature range of almost 103 °C at the back of the cladding, and still 78.2 °C at the wind barrier. This sensor also recorded the largest change between two consecutive measurements with 37.5 °C. But significant differences between two consecutive measurements were also found at the walls, e.g., *TS2-3* with 31.3 °C, *TW3-3* with 27.0 °C, or *TE4-3* with 24.3 °C. According to ISO 15686-1 on *Buildings and constructed assets - Service life planning*, "*extreme levels or fast alterations of temperature"* are among the most common agents affecting the service life of building materials and components. High temperatures are of particular importance, as they increase the reactivity of carbon atoms with oxygen in plastics, followed by further decomposition and reaction of the initial products through many stages [9].

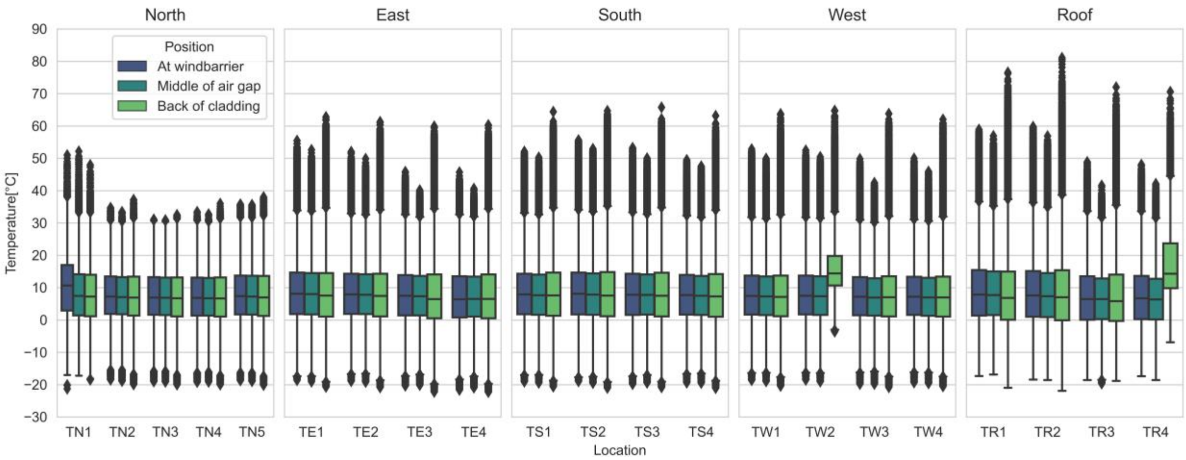

Figure 4. Boxplots of temperature in the air gaps of the different building envelopes at the ZEB Laboratory. Due to sensor malfunctions, there is incomplete data for TN1-1, TE4-2, TE4-3, TW2-3, and TR4-3.

Figure 5 presents time percentage of the average surface temperature at the wind barrier at the different building envelopes. These have been categorised in time-intervals of 5 °C steps. With 22.5 % on average, the wind barrier surface temperature has mostly been in the temperature interval between 0 and 5 °C. In 60.2 % of the 2-year measurement period from September 2020 to August 2022 it has been between 0 and 15 °C. Moreover, the roof and the façade to the south have the highest share of hours in the temperature categories of 25 °C and above. The surface temperature at the northern façade, on the other hand, rarely rises above 30 °C.

Table 1 shows the distribution of hours in the same time intervals of all sensors at the wind barrier during the measurement period. At the northern façade, the temperature exceeds 40 °C only at the uppermost sensor (*TN1-1*), where the façade is unshaded especially in the morning and evening of the long summer days at Trondheim's latitude. Due to a large building to the West of the ZEB Laboratory (see also figure 1a on the left), there are comparatively few hours in which high temperatures are recorded on the western façade. Contrary to this, the largely unshaded façade to the East, where solar irradiance is strongest during the morning hours, has a larger share of measured temperatures above 15 °C. As might be expected, the roof and the façade facing South have the largest share of measured temperatures in the upper six temperature intervals. It is noticeable, however, that at the roof there are considerably more hours within the temperature interval between -5 and 0 °C, while there are significantly less in the 5–10 °C interval. This can be explained by longwave radiation losses from the roof to the sky especially during clear nights so that lower temperatures are recorded than at the less exposed vertical facades.

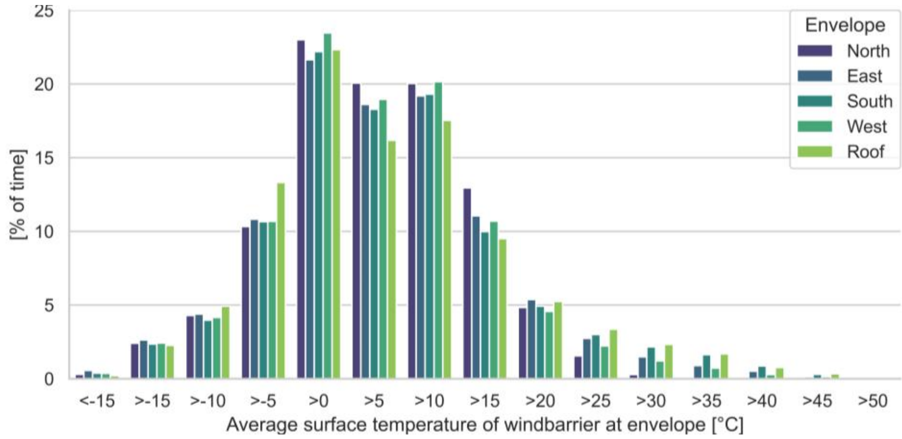

Figure 5. Time percentage of average surface temperature at the wind barrier in the temperature categories at the different building envelopes during the two years of measurements (Sep 2020–Aug 2022).

Table 1. Time distribution in the temperature intervals [°C] of the sensors at the surface of the wind barrier in hours (rounded).

Sensor	<-15	>-15	>-10	>-5	>0	>5	>10	>15	>20	>25	>30	>35	>40	>45	>50	>55
TN1-1[a]	5	85	331	1135	2641	2043	2698	2364	1101	448	167	61	10	5	0	0
TN2-1	47	394	721	1825	4137	3461	3607	2268	787	244	29	0	0	0	0	0
TN3-1	63	459	743	1891	4190	3393	3610	2250	736	178	6	0	0	0	0	0
TN4-1	77	458	833	1945	4189	3363	3559	2155	736	187	19	0	0	0	0	0
TN5-1	48	399	746	1883	4074	3350	3458	2294	903	306	57	3	0	0	0	0
TE1-1	51	435	714	1839	3765	3195	3322	1929	1036	537	270	186	131	81	27	0
TE2-1	56	396	713	1817	3828	3330	3373	1930	983	500	259	168	117	47	1	0
TE3-1	134	482	789	1929	3824	3256	3389	1955	896	457	239	128	44	1	0	0
TE4-1	203	487	822	2007	3822	2828	2976	1756	801	425	227	111	35	0	0	0
TS1-1	61	392	685	1840	3895	3239	3392	1729	872	541	376	294	149	51	7	0
TS2-1	56	393	696	1870	3834	3134	3320	1704	856	556	384	313	248	126	32	2
TS3-1	95	432	716	1885	3856	3180	3369	1738	835	522	373	286	165	60	10	0
TS4-1	70	431	717	1838	3951	3256	3513	1801	843	491	336	184	75	15	0	0
TW1-1	52	388	720	1864	4079	3361	3455	1841	792	377	240	187	112	46	8	0
TW2-1	50	391	696	1838	4107	3344	3474	1865	800	400	237	182	95	39	5	0
TW3-1	93	453	752	1910	4098	3340	3605	1894	734	321	162	100	44	17	0	0
TW4-1	72	451	740	1881	4134	3297	3655	1945	742	310	151	90	39	13	0	0
TR1-1	23	266	705	2067	4129	2739	2988	1786	1021	648	430	312	241	104	51	12
TR2-1	43	340	763	2246	3923	2794	2961	1669	985	629	426	315	240	108	60	18
TR3-1	121	498	971	2641	3677	2907	3099	1561	848	550	391	174	74	10	0	0
TR4-1	106	419	1030	2340	3888	2935	3157	1599	863	564	389	159	66	6	0	0

[a] Incomplete data (September 2020–April 2021 is missing)

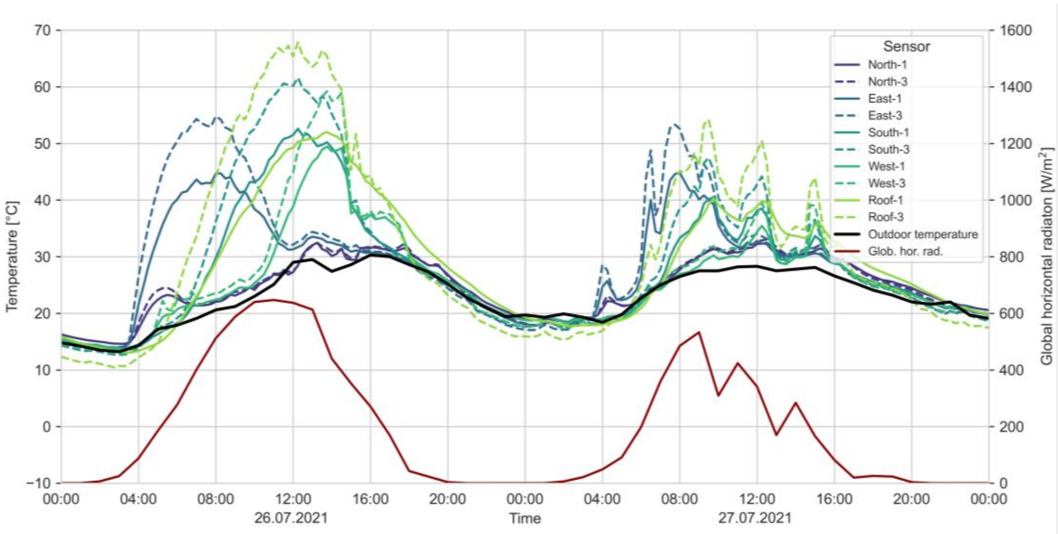

Figure 6. Average surface temperatures of the wind barrier (solid lines) and at the back of the cladding (dashed lines) of all sensors of the different envelopes for the two days with the highest outdoor air temperature during the measurement period (July 26–27, 2021). Outdoor air temperature (black line) and global horizontal radiation (red line) are hourly values and measured in 70 m distance to the studied building.

In figure 6, the measured surface temperatures at the wind barrier and at the back of the cladding are shown for the two warmest days of the measurement period. It is clearly visible, that the temperatures at the back of the cladding are surpassing those at the wind barrier during the day, while they are slightly lower during the night. During the morning hours, especially the façade to the East experiences a strong increase in temperatures. Also, at the façade to the North, a peak in temperatures at the sensor positions can be seen on both days in the morning. On both days, the highest temperatures are recorded at the roof at the back of the cladding. Especially on the second day, it is clearly noticeable how the temperatures in the air gap follow the pattern of solar irradiation that due to cloud coverage is less uniform than on the first day. In Table 2, the largest negative and largest positive difference as well as the median of the difference between the measured temperatures in the air gap and the outdoor air temperature is shown. The results are presented as envelope surface averages, meaning that all sensor data of a particular position (wind barrier, cladding, or wind barrier) are averaged per building envelope surface orientation. The differences can reach up to about 47 °C and can get as low as -13.3 °C at the roof. In the air gap of the façade to the North, the measured temperatures are closest to the outdoor air temperature.

Table 2. Median, largest negative and largest positive difference between the measured envelope surface-averaged temperatures in the air gap (T_{sensor}) and the outdoor air temperature (T_{out}).

Envelope surface	Position	$min(T_{sensor} - T_{out})$	$max(T_{sensor} - T_{out})$	Median
North	Wind barrier	-9.2	11.8	0.3
	Cladding	-9.8	14.8	-0.2
East	Wind barrier	-10.3	28.8	-0.1
	Cladding	-11.1	41.5	-0.6
South	Wind barrier	-10.3	30.1	0.0
	Cladding	-11.4	45.0	-0.6
West	Wind barrier	-10.0	23.3	0.0
	Cladding	-10.9	36.3	-0.5
Roof	Wind barrier	-10.6	27.7	-0.1
	Cladding	-13.3	46.8	-1.1

4. Conclusions

The measurements provide valuable insights to the microclimatic conditions in ventilated air gaps and the in-use conditions of air-tightening materials. They are publicly accessible and can be accessed here: https://zenodo.org/record/7042548 [10]. The results can be used to better design accelerated ageing and durability tests of these materials. To accurately predict the service life of building components, ISO 15686-1 [11] suggests that ideally, "*[…] the microclimate [and] the performance of the component under the intended conditions […]*" should be known and that this data is not often available. The ongoing work described in this paper aims to fill the knowledge gap regarding these conditions for materials adjacent to or in the ventilated air gap of highly insulated wood frame walls with wood, Alu-PE panels, and BIPV as cladding, as well as BIPV-covered roofs. The presented results are expected to provide useful information for developing durable materials for conditions to be expected in ventilated air gaps in the investigated, subarctic climate of Trondheim, Norway. Particularly, the large temperature range and rapid changes in temperature over relatively short periods of time put significant strain on plastics that are often used as tightening materials. Further measurements and studies should be performed in other locations around the world for a more complete understanding of the exposure of such materials.

Acknowledgements

The authors gratefully acknowledge the financial support by the Research Council of Norway and several partners through the TightEN project [grant number 294894], the Centre of Research-based Innovation Klima 2050 (www.klima2050.no) [grant number 237859], and the ZEB Laboratory project [grant number 245663].

References

[1] Girma G M and Tariku F 2021 *Build. Environ.* **194** 107710.
[2] Riahinezhad M, Eve A, Armstrong M, Collins P and Masson J-F 2019 *Can. J. Civ. Eng.* **46** 969.
[3] Geving S, Erichsen T H, Nore K and Time B 2006 *Hygrothermal conditions in wooden claddings. Test house measurements* (Oslo, Norway).
[4] Rüther P, Oksavik O, Nocente A and Gullbrekken L 2021 *J. Phys.: Conf. Ser.* **2069** 12200.
[5] Brozovsky J, Nocente A and Rüther P 2022 *Build. Environ.* **228** 109917.
[6] Nocente A, Time B, Mathisen H M, Kvande T and Gustavsen A 2021 *J. Phys.: Conf. Ser.* **2069** 12109.
[7] Time B, Engebø A, Christensen M, Dalby O and Kvande T 2019 *IOP Conf. Ser.: Earth Environ. Sci.* **352** 12053.
[8] Time B, Mathisen H M, Førland-Larsen A, Ramberg Myhr A., Jacobsen T and Gustavsen A 2019 *ZEB Laboratory - Research Possibilities* (Oslo).
[9] Pickett J E 2018 *Handbook of environmental degradation of materials* ed M Kutz (Norwich: William Andrew) pp 163–84.
[10] Rüther P and Oksavik O 2022 *TightEN - ZEB-Laboratory - Temperature behind cladding.* Available at https://doi.org/10.5281/zenodo.7042548.
[11] ISO 15686-1 2011 *Buildings and constructed assets - Service life planning. Part 1: General principles and framework* (Geneva, Switzerland).